

An empirical Bayes approach to stochastic blockmodels and graphons: shrinkage estimation and model selection

Zhanhao Peng, Qing Zhou

Department of Statistics, University of California, Los Angeles, USA

Abstract

The graphon (W-graph), including the stochastic block model as a special case, has been widely used in modeling and analyzing network data. This random graph model is well-characterized by its graphon function, and estimation of the graphon function has gained a lot of recent research interests. Most existing works focus on detecting the latent space of the model, while adopting simple maximum likelihood or Bayesian estimates for the graphon or connectivity parameters given the identified latent variables. In this work, we propose a hierarchical model and develop a novel empirical Bayes estimate of the connectivity matrix of a stochastic block model to approximate the graphon function. Based on the likelihood of our hierarchical model, we further introduce a new model selection criterion for choosing the number of communities. Numerical results on extensive simulations and two well-annotated social networks demonstrate the superiority of our approach in terms of estimation accuracy and model selection.

Source codes and datasets are available at <https://github.com/chandler96/EBgraph>.

1. Introduction

Network data, consisting of relations among a set of individuals, are usually modeled by a random graph. Each individual corresponds to a vertex or node in the graph, while their relations are modeled by edges between the vertices. Such data have become popular in many domains, including biology, sociology and communication (Albert and Barabási 2002). Statistical methods are often used to analyze network data so that the underlying properties of the network structure can be better understood via estimation of model parameters. Examples of such properties include degrees, clusters and diameter (Barabási and Albert 1999, Newman et al. 2002) among others.

¹Corresponding author (Qing Zhou). Email: zhou@stat.ucla.edu

To better understand the heterogeneity among vertices in a network, community detection and graph clustering methods (Girvan and Newman 2002, Newman 2004) have been proposed to group vertices into clusters that share similar connection profiles. A large portion of the clustering methods are developed based on the stochastic block model (SBM) (Freeman 1983), which constructs an interpretable probabilistic model for the heterogeneity among nodes and edges in an observed network.

For a simple random graph on n nodes or vertices, the relationships between the nodes are modeled by $\frac{1}{2}n(n-1)$ binary random variables representing the presence or absence of an edge. The edge variables can be equivalently represented by an $n \times n$ adjacency matrix \mathbf{X} , where $X_{ij} = 1$ if node i and j are connected and $X_{ij} = 0$ otherwise. We do not consider self loops in this work, and thus $X_{ii} = 0$ for $i = 1, \dots, n$.

Many popular graph models (Lloyd et al. 2012) make exchangeability assumption on the vertices: The distribution of the random graph is invariant to permutation or relabeling of the vertices. A large class of exchangeable graphs can be defined by the so-called *graphon* function (Lovasz and Szegegy 2006). A graphon $W(u, v)$ is a symmetric function: $[0, 1]^2 \rightarrow [0, 1]$. To generate an n -vertex random graph given a graphon $W(u, v)$, we first draw latent variables u_i from the uniform distribution $U(0, 1)$ for $i = 1, \dots, n$ independently. Then we connect each pair of vertices (i, j) with probability $W(u_i, u_j)$, i.e.

$$\mathbb{P}(X_{ij} = 1 | u_i, u_j) = W(u_i, u_j), \quad i, j = 1, \dots, n. \quad (1)$$

In particular, the stochastic block model mentioned above can be seen as a special case of the graphon model, where $W(u, v)$ is a piecewise constant function. Abbe (2018) has summarized recent developments on the model. Under an SBM, the vertices are randomly labeled with independent latent variables $\mathbf{Z} = (z_1, \dots, z_n)$, where $z_i \in \{1, \dots, K\}$ for $i = 1, \dots, n$ and K is the number of communities or clusters among all the nodes. The distribution of (\mathbf{Z}, \mathbf{X}) is specified as follows:

$$\begin{aligned} \mathbb{P}(z_i = m) &= \pi_m, \quad m \in \{1, \dots, K\}, i = 1, \dots, n, \\ \mathbb{P}(X_{ij} = 1 | z_i, z_j) &= \theta_{z_i z_j}, \quad i, j = 1, \dots, n, \end{aligned} \quad (2)$$

where $\sum_m \pi_m = 1$ and each $\theta_{km} \in [0, 1]$. Put $\pi = (\pi_1, \dots, \pi_m)$ and $\Theta = (\theta_{ij})_{K \times K}$.

Many efforts have been made on statistical inference of the SBM to detect block structures as well as to estimate the connectivity probabilities in the blocks. Some classical and popular methods include MCMC, degree-based algorithms and variational inference among other. Nowicki and Snijders (2001) developed a Gibbs sampler to estimate parameters for graphs of small sizes (up to a few hundred nodes). A degree-based algorithm (Channarond et al. 2012) achieves classifica-

tion, estimation and model selection from empirical degree data. The variational EM algorithm (Daudin et al. 2008) and variational Bayes EM (Latouche et al. 2012) approximate the conditional distribution of group labels given the network data by a class of distributions with simpler forms. Suwan et al. (2016) recast the SBM to a random dot product graph (Young and Scheinerman 2007) and developed a Bayesian inference method with a prior specified empirically by adjacency spectral embedding.

Due to higher model complexity, estimating a graphon is challenging. Some works (Airoldi et al. 2013, Olhede and Wolfe 2014, Latouche and Robin 2016) have focused on the nonparametric perspective of this model and developed methods to estimate a graphon based on SBM approximation. These methods estimate a graphon function by partitioning vertices and computing the empirical frequency of edges across different blocks. Many algorithms put emphasis on model selection (Airoldi et al. 2013) or bandwidth determination (Olhede and Wolfe 2014). Latouche and Robin (2016) proposed a variational Bayes approach to graphon estimation and used model averaging to generate a smooth estimate.

After the block structure of a network is identified, most of the above methods simply use the empirical connection probability within and between blocks to estimate Θ . When the number of nodes in a block is too small, the estimate can be highly inaccurate with a large variance. Latouche and Robin (2016) developed an alternative method under a Bayesian framework, where they put conjugate priors on the parameters (π, Θ) . In particular, they assume $\theta_{ab} \sim \text{Beta}(\alpha_{ab}, \beta_{ab})$ independently for $a, b \in \{1, \dots, K\}$, where the parameters $(\alpha_{ab}, \beta_{ab})$ in the prior are chosen *in priori*. Similar to the MLE, the connection probability θ_{ab} of each block is estimated separately and thus may suffer from the same high variance issue for blocks with a smaller number of nodes. To alleviate this difficulty, we propose a hierarchical model for network data to borrow information across different blocks. Under this model, we develop an empirical Bayes estimator for $\Theta = (\theta_{ab})$ and a model selection criterion for choosing the number of blocks. Empirical Bayes method is usually seen to have better performance when estimating many similar and variable quantities (Efron 2010). This inspires our proposal as the connection probabilities can be similar across many different communities. By combining data from many blocks, estimates will be much more stable even if the number of nodes is small in each block.

In summary, our method has two major novel components: 1) shrinkage estimation for connectivity parameters, and 2) a novel likelihood-based model selection criterion, both under our proposed hierarchical model. As demonstrated by extensive simulations and experiments on real-world data, these contributions give us substantial gain in estimation accuracy and model selection performance, especially for graphons. Moreover, our method is very easy to implement and does not cost much extra computational resources compared to existing approaches.

The paper is organized as follows. In Section 2, we will develop our empirical Bayes method for the SBM and the graphon, focusing on connection probability estimation and model selection on the number of blocks. Then we will compare the performance of our methods with other existing methods on simulated data in Section 3 and on two real-world networks in Section 4. The paper is concluded with a brief discussion. Some technical details and additional numerical results are provided in the Supplementary Material.

2. An Empirical Bayes Method

Let us first consider the SBM. After the vertices of an observed network have been partitioned into clusters by a graph clustering algorithm, we develop an empirical Bayes estimate of the connection probability matrix Θ based on a hierarchical Binomial model. Under this framework, we further propose a model selection criterion to choose the number of blocks. Our method consists of three steps:

- **Graph clustering** For a network with n vertices, cluster the vertices into K blocks by a clustering algorithm. Let $Z : [n] \rightarrow [K]$ denote the cluster assignment, where $[m] := \{1, \dots, m\}$ for an integer m .
- **Parameter estimation** Given Z , we find an empirical Bayes estimate $\hat{\Theta}_{\text{EB}} = (\hat{\theta}_{ij}^{\text{EB}})_{K \times K}$ by estimating the hyperparameters of the hierarchical binomial model.
- **Model Selection** Among multiple choices of K , we select the \hat{K} that maximizes a penalized marginal likelihood under our hierarchical model.

In Section 2.3, we generalize our method to the graphon model, following the idea of SBM approximation to a graphon.

Algorithms to detect blocks of a stochastic block model have been widely studied, including spectral clustering by [Rohe et al. \(2011\)](#), Monte Carlo sampling by [Nowicki and Snijders \(2001\)](#) and variational approximations by [Daudin et al. \(2008\)](#). As an extension to the work of [Daudin et al. \(2008\)](#), [Latouche et al. \(2012\)](#) proposed a variational Bayes approximation to the posterior distribution of the parameters (π, Θ) and of the latent cluster labels \mathbf{Z} (Section S1.1 in Supplementary Material for a more detailed review). Given the \mathbf{Z} estimated by their approach, we will develop our hierarchical model and empirical Bayes estimates.

2.1. Estimating connection probabilities

In this subsection, we consider the SBM and assume a partition $Z : [n] \rightarrow [K]$ of the nodes is given, where K is the number of blocks. Note that $Z^{-1}(a)$ for

$a \in [K]$ is the subset of nodes in the a -th cluster. Let

$$B_{ab} = \{(i, j) : (i, j) \in Z^{-1}(a) \times Z^{-1}(b), i < j\}$$

be the collection of node pairs in the (i, j) th block. According to the SBM, the connection probability between any $(i, j) \in B_{ab}$ is θ_{ab} . Recall that $\mathbf{X} = (X_{ij})$ is the observed adjacency matrix. Let $X_{ab}^B = \sum_{(i,j) \in B_{ab}} X_{ij}$ be the number of edges in block (a, b) . Then, we have

$$X_{ab}^B | \theta_{ab} \sim \text{Binomial}(n_{ab}, \theta_{ab}), \quad (3)$$

where $n_{ab} = |B_{ab}| = |Z^{-1}(a)| \cdot |Z^{-1}(b)|$ for $a \neq b$ and $n_{aa} = |Z^{-1}(a)| \cdot (|Z^{-1}(a)| - 1)/2$ as self loops are not allowed. Based on the empirical frequency of edges in the block (a, b) , we have an MLE for the edge connection probability

$$\hat{\theta}_{ab}^{\text{MLE}} = \frac{X_{ab}^B}{n_{ab}}, \quad a, b \in \{1, \dots, K\}. \quad (4)$$

When K is large, the number of nodes, and thus n_{ab} , in some blocks will be small, which leads to a high variance of the MLE. To stabilize the estimates, we may borrow information across blocks to improve estimation accuracy. To do this, we set up a hierarchical model by putting conjugate prior distributions on θ_{ab} . To accommodate the heterogeneity in θ_{ab} , we use two sets of hyperparameters so that the within and between-block connectivities are modeled separately:

$$\theta_{ab} | (\alpha_d, \beta_d) \sim \text{Beta}(\alpha_d, \beta_d), \quad a, b \in \{1, \dots, K\}, \quad (5)$$

where $d = 0$ for $a = b$ and $d = 1$ for $a \neq b$, i.e. the diagonal and off-diagonal elements of the connectivity matrix Θ follow $\text{Beta}(\alpha_0, \beta_0)$ and $\text{Beta}(\alpha_1, \beta_1)$, respectively. The prior distribution (5) together with (3) defines the distribution $[\mathbf{X}, \Theta | (\alpha_d, \beta_d)_{d=0,1}]$. Here (α_d, β_d) , $d = 0, 1$, are hyperparameters to be estimated by our method. A diagram of our model is shown in Figure 1. Note that the use of two sets of hyperparameters is in line with common assumptions of the stochastic block model, such as assortativity (Danon et al. 2005) or disassortativity, i.e. within-group connectivities are different than between-group connectivities.

The conditional posterior distribution of θ_{ab} given $(X_{ab}^B, \alpha_d, \beta_d)$ is

$$\theta_{ab} | (X_{ab}^B, \alpha_d, \beta_d) \sim \text{Beta}(\alpha_d + X_{ab}^B, \beta_d + n_{ab} - X_{ab}^B),$$

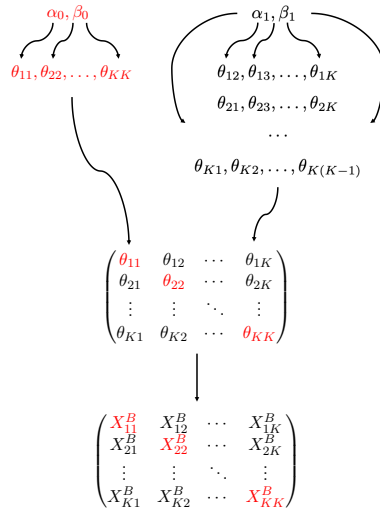


Figure 1 – A diagram of the hierarchical model. The connectivity parameters θ_{ab} , $a, b \in \{1, \dots, K\}$, follow beta distributions of two sets of hyperparameters, i.e. (α_0, β_0) for diagonal blocks (red) and (α_1, β_1) for off-diagonal blocks, and the number of edges X_{ab}^B in a block, depends on θ_{ab} as in (3).

and the conditional posterior mean of θ_{ab} is

$$\begin{aligned} \hat{\theta}_{ab}^{\text{EB}}(\alpha_d, \beta_d) &\equiv \mathbb{E}(\theta_{ab} | X_{ab}^B, \alpha_d, \beta_d) \\ &= \frac{\alpha_d + X_{ab}^B}{\alpha_d + \beta_d + n_{ab}} = \eta_{ab} \frac{\alpha_d}{\alpha_d + \beta_d} + (1 - \eta_{ab}) \frac{X_{ab}^B}{n_{ab}}, \end{aligned} \quad (6)$$

for $a, b \in \{1, \dots, K\}$, where

$$\eta_{ab} = \frac{\alpha_d + \beta_d}{\alpha_d + \beta_d + n_{ab}} \in [0, 1] \quad (7)$$

is the shrinkage factor that measures the amount of information borrowed across blocks. When the variance among θ_{ab} across the blocks is high, α_d and β_d will be estimated to be small. Thus, η_{ab} will be close to 0 so that the estimate $\hat{\theta}_{ab}^{\text{EB}}$ will be close to $\hat{\theta}_{ab}^{\text{MLE}}$. When the variance among θ_{ab} is low, our estimates of α_d and β_d will be large, the shrinkage factor approaches 1, and eventually $\hat{\theta}_{ab}^{\text{EB}}$ will become identical across all blocks. In this case, we are essentially pooling data in all blocks to estimate θ_{ab} . Generally speaking, the shrinkage factor η_{ab} is determined by the data through the estimation of the hyperparameters (α_d, β_d) , and it leads to a good compromise between the above two extreme cases.

Given the partition Z from a graph clustering algorithm, we maximize the marginal likelihood of the observed adjacency matrix \mathbf{X} to estimate the hyper-parameters (α_d, β_d) for $d = 0, 1$. Let \mathbf{X}_{ab} denote the adjacency submatrix for nodes in the block (a, b) defined by the partition Z . Integrating over Θ , the marginal log-likelihood function for the diagonal blocks is

$$\begin{aligned}\mathcal{L}(\alpha_0, \beta_0 | \mathbf{X}, Z) &= \sum_{a=1}^K \log \mathbb{P}(\mathbf{X}_{aa} | \alpha_0, \beta_0) \\ &= \sum_{a=1}^K \log \int_{\theta_{aa}} \mathbb{P}(\mathbf{X}_{aa} | \theta_{aa}) p(\theta_{aa} | \alpha_0, \beta_0) d\theta_{aa} \\ &= \sum_{a=1}^K \log \text{Beta}(\alpha_0 + X_{aa}^B, \beta_0 + n_{aa} - X_{aa}^B) - K \log \text{Beta}(\alpha_0, \beta_0),\end{aligned}\tag{8}$$

where $\text{Beta}(x, y) = \int_0^1 t^{x-1} (1-t)^{y-1} dt$ is the beta function. Similarly, the marginal log-likelihood function for the off-diagonal blocks is

$$\begin{aligned}\mathcal{L}(\alpha_1, \beta_1 | \mathbf{X}, Z) &= \sum_{a < b} \log \text{Beta}(\alpha_1 + X_{ab}^B, \beta_1 + n_{ab} - X_{ab}^B) - \frac{1}{2} K(K-1) \log \text{Beta}(\alpha_1, \beta_1).\end{aligned}\tag{9}$$

We find the maximum likelihood estimates of the hyper parameters, i.e.

$$(\hat{\alpha}_d, \hat{\beta}_d) = \arg \max_{\alpha_d, \beta_d} \mathcal{L}(\alpha_d, \beta_d | \mathbf{X}, Z),\tag{10}$$

for $d = 0, 1$. Then we can estimate Θ by plugging the MLE of the hyper-parameters in (10) into (6), i.e.

$$\hat{\theta}_{ab}^{\text{EB}} = \begin{cases} \hat{\theta}_{aa}^{\text{EB}}(\hat{\alpha}_0, \hat{\beta}_0), & a = b \\ \hat{\theta}_{ab}^{\text{EB}}(\hat{\alpha}_1, \hat{\beta}_1), & a \neq b \end{cases}.\tag{11}$$

Since the hyper-parameters are estimated by using all blocks, our empirical Bayes estimates of θ_{ab} also make use of information from all data to improve the accuracy. Though (10) does not have a closed form solution, we can use an optimization algorithm such as bounded limited-memory BFGS (L-BFGS-B) (Byrd et al. 1995) to find the maximizer. As shown in Figure S2 in Supplementary Material for a typical dataset, the global maximizers can be easily found.

Suwan et al. (2016) developed a different empirical Bayesian method for SBMs under a random dot product graph formulation. They introduce K latent positions, $\nu_1, \dots, \nu_K \in \mathbb{R}^d$, and define the connection probabilities by inner products

between the latent positions, $\theta_{ab} = \langle \nu_a, \nu_b \rangle$ for $1 \leq a, b \leq K$. The prior distribution for ν_k is a multivariate Gaussian distribution $\nu_k \sim \mathcal{N}_d(\hat{\mu}_k, \hat{\Sigma}_k)$. In particular, the parameters $\hat{\mu}_k, \hat{\Sigma}_k$ in the prior are chosen by Gaussian mixture modeling of pre-estimated latent positions obtained via adjacency spectral embedding. Thus, these prior distributions are called *empirical* priors and they are used to model the uncertainty in the latent positions ν_1, \dots, ν_K . In our method, the hyperparameters (α, β) in the beta prior distributions are not pre-estimated by a separate method, but instead are estimated under a coherent hierarchical model. In addition to modeling uncertainty in the connectivity probabilities θ_{ab} , the hyperparameters also lead to information sharing via shrinkage.

2.2. Selecting partitions

So far we have regarded the number of blocks K as given in our empirical Bayes method. The choice of K will certainly impact the performance of our method. If K is too small, for SBM many blocks will not be identified, and for graphon the approximated function will only have a small number of constant pieces, both leading to highly biased estimates. On the other hand, if K is too big, the number of vertices in each block will be very small, resulting in high variances. Thus, it is important to select a proper number of blocks to achieve the best estimation accuracy.

Our empirical Bayes approach under the hierarchical model also provides a useful criterion for this model selection problem. Note that (8) and (9) define the conditional likelihood of \mathbf{X} given the hyperparameters (α_d, β_d) and the partition Z input from a graph clustering algorithm. We can compare this likelihood for different input partitions and select the best one.

Suppose we have m candidate partition schemes Z_1, \dots, Z_m . Denote the corresponding number of communities by K_1, \dots, K_m . Our goal is to choose the optimal partition that maximizes the joint likelihood of the observed adjacency matrix \mathbf{X} and the partition Z with a penalty on the model complexity. To do this, we include Z in our model as in (2) and put a Jeffreys prior (Jeffreys 1946) on π , i.e.

$$\pi \sim \text{Dirichlet}(\tau_1, \dots, \tau_K), \quad \tau_1 = \dots = \tau_K = 1/2.$$

For a partition Z with K communities, the joint likelihood of \mathbf{X} and Z given the

hyper-parameters $(\alpha_0, \alpha_1, \beta_0, \beta_1)$ is

$$\begin{aligned}
& \mathbb{P}(\mathbf{X}, Z | \alpha_0, \alpha_1, \beta_0, \beta_1) \\
&= \mathbb{P}(\mathbf{X} | Z, \alpha_0, \alpha_1, \beta_0, \beta_1) \int \mathbb{P}(Z | \pi) p(\pi) d\pi \\
&= \mathbb{P}(\mathbf{X} | Z, \alpha_0, \alpha_1, \beta_0, \beta_1) \frac{\Gamma(\sum_{i=1}^K \tau_i) \prod_{i=1}^K \Gamma(n_i + \tau_i)}{\Gamma(n + \sum_{i=1}^K \tau_i) \prod_{i=1}^K \Gamma(\tau_i)},
\end{aligned} \tag{12}$$

after marginalizing out the parameter π , where n_i is the number of nodes in cluster i defined by the partition Z . Maximizing over the hyperparameters leads to the MLE $(\hat{\alpha}_0, \hat{\alpha}_1, \hat{\beta}_0, \hat{\beta}_1)$ defined in (10). Evaluating the likelihood (12) at the estimated hyperparameters, we define the goodness-of-fit part for our model selection criterion as

$$\begin{aligned}
J_Z &= \log \mathbb{P}(\mathbf{X}, Z | \hat{\alpha}_0, \hat{\alpha}_1, \hat{\beta}_0, \hat{\beta}_1) \\
&= \sum_{d \in \{0,1\}} \mathcal{L}(\hat{\alpha}_d, \hat{\beta}_d | \mathbf{X}, Z) + \log \frac{\Gamma(\sum_{i=1}^K \tau_i) \prod_{i=1}^K \Gamma(n_i + \tau_i)}{\Gamma(n + \sum_{i=1}^K \tau_i) \prod_{i=1}^K \Gamma(\tau_i)},
\end{aligned} \tag{13}$$

where $\mathcal{L}(\hat{\alpha}_d, \hat{\beta}_d | \mathbf{X}, Z)$ is as in (8) and (9) for $d = 0, 1$. Following the ICL-like (integrated complete likelihood) criterion in [Mariadassou et al. \(2010\)](#), we add two penalty terms to control model complexity: The first term corresponds to a penalty on the number of parameters in π and the second the number of parameters in Θ . Therefore, our model selection criterion is to choose the partition

$$\hat{Z} = \arg \max_{Z \in \{Z_1, \dots, Z_m\}} \left\{ J_Z - \frac{1}{2} \left[(K-1) \log n + \frac{K(K+1)}{2} \log \frac{n(n-1)}{2} \right] \right\}, \tag{14}$$

where K is the number of clusters defined by the partition Z . As we have mentioned in the introduction, there are quite a few graph clustering algorithms, and the performance of many of them is highly dependent on the input number of partitions. Our criterion for selecting the number of clusters applies to any method used for the node clustering step, and thus it protects our method from inferior input node clustering results. The ICL model selection criterion (14) is indeed an approximation to the marginal likelihood $\mathbb{P}(\mathbf{X} | K)$ ([Mariadassou et al. 2010](#)). The joint likelihood depends on the EB estimates of the hyperparameters, which is unique to our hierarchical model. While the VBEM criterion ([Latouche et al. 2012](#)) uses a standard SBM likelihood without a hierarchical structure nor estimation of priors. We can easily apply other penalty terms in various model selection criteria to our likelihood, and fully expect similar behavior in terms of selecting the number of clusters, since most of them approximate in some way the marginal likelihood or the Bayes factor.

2.3. Graphon estimate

Now we assume that the true model is a graphon as in (1). We use an SBM with K blocks as an approximation to the graphon, i.e., we approximate $W(u, v)$ by a piecewise constant function: We divide the unit interval $[0, 1]$ into K pieces based on π so that the length of the k -th piece is π_k . Let the endpoints of these pieces be $c_k = \sum_{i=1}^k \pi_i$ for $k = 1, \dots, K$ and put $c_0 \equiv 0$. Then the graphon function defined on $[0, 1] \times [0, 1]$ is approximated by a $K \times K$ blockwise constant function,

$$\widetilde{W}(u, v) = \theta_{ab} \quad \text{if } (u, v) \in [c_{a-1}, c_a) \times [c_{b-1}, c_b).$$

To estimate a graphon W , we first run a clustering algorithm to estimate a partition Z and then apply the empirical Bayes method to obtain $\hat{\theta}_{ab}^{\text{EB}}$. Let n_k denote the size of the k -th cluster of vertices. We calculate its proportion to estimate π_k by $\hat{\pi}_k = n_k/n$ and compute the cumulative proportion $\hat{c}_k = \sum_{i=1}^k \hat{\pi}_i$ for $k = 1, \dots, K$. Define a binning function,

$$\text{bin}(x) = 1 + \sum_{k=1}^K \mathbb{I}(c_k \leq x), \quad (15)$$

and the graphon W is then estimated by

$$\widehat{W}(x, y) = \hat{\theta}_{\text{bin}(x), \text{bin}(y)}^{\text{EB}}, \quad x, y \in [0, 1]. \quad (16)$$

As shown by [Bickel and Chen \(2009\)](#), the graphon is not identifiable in the sense that any measure-preserving transformation on $[0, 1]$ will define an equivalent random graph. Following their method, imposing the constraint that

$$g(x) = \int_0^1 W(x, y) dy$$

is nondecreasing leads to identifiability. For SBM approximation, the corresponding constraint is that

$$g(l) = \sum_{k=1}^K \pi_k \theta_{lk} \quad (17)$$

is nondecreasing in l . This constraint can be satisfied by relabeling the K clusters of nodes.

As for the SBM, selecting a proper number of clusters K is important for the estimation of a graphon. We will apply the same model selection criterion (14) to choose the optimal partition Z and the associated K among a collection of

partitions.

3. Results on simulated graphs

In this section we present numerical results on graphs simulated from stochastic block models and graphon functions. We compare our method with other existing methods in terms of estimating connection probabilities (Section 2.1) and model selection for choosing the number of clusters (Section 2.2).

For stochastic block models, we compare our estimated connectivity matrix $\widehat{\Theta}_{\text{EB}}$ (11) to the maximum likelihood estimate $\widehat{\Theta}_{\text{MLE}}$ as in (4) and the variational Bayes inference $\widehat{\Theta}_{\text{VBEM}}$ from Latouche et al. (2012). Variational Bayes inference provides a closed-form approximate posterior distribution for (π, Θ) by minimizing the KL divergence between an approximated and the underlying distributions of $[Z | \mathbf{X}]$. It constructs point estimates for the parameters based on EM iterations (Section S1.1, Supplementary Material). We compute the mean squared error (MSE)

$$\text{MSE} = \frac{1}{n(n-1)} \sum_{i=1}^n \sum_{j \neq i} (\widehat{\Theta}'_{ij} - \Theta'_{ij})^2 \quad (18)$$

of an estimated $n \times n$ connection probability matrix $\widehat{\Theta}'$. Here, $\Theta' = (\Theta_{ij})_{n \times n}$ is the true connection probability matrix among the n nodes, i.e. $\Theta'_{ij} = \theta_{ab}$ if $Z^*(i) = a$ and $Z^*(j) = b$ for $i, j = 1, \dots, n$, where Z^* is the true partition, and $\widehat{\Theta}'_{ij} = \widehat{\theta}_{ab}$ if $Z(i) = a$ and $Z(j) = b$. For graphons, $\widehat{W}(x, y)$ is estimated by SBM approximation as in Section 2.3, and correspondingly the MSE is calculated as

$$\text{MSE} = \int \int_0^1 (W(x, y) - \widehat{W}(x, y))^2 dx dy. \quad (19)$$

Due to the nonidentifiability of graphons, the MSE is calculated after relabeling node clusters based on the constraint (17) to make \widehat{W} comparable to W .

We compare our model selection criterion (14) to the variational Bayes method developed by Latouche et al. (2012) (VBEM) and the cross validation risk of precision parameter (CVRP) in Airoldi et al. (2013). The CVRP is defined as

$$\mathcal{J}_{\text{CVRP}}(K) = \frac{2K}{n-1} - \frac{(n+1)K}{n-1} \sum_{i=1}^K \left(\frac{n_i}{n}\right)^2, \quad (20)$$

where n_i is the number of vertices in group i . Then, the number of clusters K is

selected by minimizing the risk $\mathcal{J}_{\text{CVRP}}$, i.e.

$$\hat{K}_{\text{CVRP}} = \arg \min_K \mathcal{J}_{\text{CVRP}}(K). \quad (21)$$

We use \mathcal{J}_{EB} , $\mathcal{J}_{\text{VBEM}}$ and $\mathcal{J}_{\text{CVRP}}$ to denote the three criteria above respectively.

3.1. Results on SBMs

We designed a constrained SBM that generates affiliation networks, i.e. two vertices within the same community connect with probability λ , and from different communities with probability $\epsilon < \lambda$. We also added a parameter $\rho \in (0, 1]$ to control the sparsity of the graph. The corresponding true connectivity matrix is

$$\Theta^* = \rho \begin{pmatrix} \lambda & \epsilon & \cdots & \epsilon \\ \epsilon & \lambda & \cdots & \vdots \\ \vdots & & \ddots & \epsilon \\ \epsilon & \cdots & \epsilon & \lambda \end{pmatrix}_{K^* \times K^*},$$

where K^* is the number of communities.

To generate dense graphs (model 1), we set $\lambda = 0.9$, $\epsilon = 0.1$, and $\rho = 1$. We generated graphs with $n = 200$ vertices and the number of communities $K^* \in \{10, 11, \dots, 18\}$. For each choice of K^* , we generated 100 networks independently. For each network, all the nodes were randomly divided into K^* clusters with equal probability $1/K^*$, and then connected according to the connectivity matrix Θ^* and their cluster labels. Note that the simulated node clusters had very different sizes, ranging between 7 and 35, due to the high variance in block size.

We also used $\lambda = 0.9$, $\epsilon = 0.1$ and $\rho = 0.2$ to generate sparse graphs (model 2), while keeping $K^* = 10$ but changing the network size $n \in \{200, 250, 300, 350, 400, 450\}$. For each network size n , we followed the same procedure as in model 1 and generated 100 networks independently.

For a simulated graph, we applied the variational Bayes algorithm (Latouche et al. 2012) with an input number of clusters $K = 1, \dots, 20$, from which we obtained K communities and a Bayesian estimate $\hat{\Theta}_{\text{VBEM}}(K)$ of the connecting probabilities among the $K \times K$ blocks. Given the estimated communities by the variational Bayes algorithm, we found $\hat{\Theta}_{\text{MLE}}(K)$ as in (4) and our empirical Bayes estimate $\hat{\Theta}_{\text{EB}}(K)$ as in (11) and compared them to the VBEM estimate. As the estimates were functions of K , so were their MSEs as defined in (18). Let $\text{MSE}_{\text{MLE}}(K)$ be the mean squared error of the MLE by plugging $\hat{\Theta}_{\text{MLE}}(K)$ into (18), where each element in $\hat{\Theta}'_{ij}$ is given by $\hat{\Theta}_{\text{MLE}}(K)$ and the partition Z . Then

we define \tilde{K} as the number of clusters that minimizes the MSE of the MLE, i.e.

$$\tilde{K} = \arg \min_K \text{MSE}_{\text{MLE}}(K) \quad (22)$$

over the input range of K . For the 100 graphs generated under the same matrix Θ^* , they share the same K^* while each one of them defines a corresponding \tilde{K} . Both K^* and \tilde{K} were used in our comparisons on model selection criteria for the number of blocks. In particular, for a general graphon, K^* may not be clearly defined and in such a case, \tilde{K} serves as the reference for comparison.

For dense graphs (model 1), as shown in Figure 2, we compared the MSEs (18) of the three estimates of Θ to the true connectivity matrix and presented the ratio of the MSE of our EB estimate to the MSEs of the MLE and VBEM estimate. For dense stochastic block models, the accuracy of MLE and that of VBEM were close, whereas EB gave better estimates for almost all K values, i.e. MSE ratios were smaller than 100%. We see a significantly smaller MSE ratio when K is close to K^* , especially when K^* is relatively small. For example, the MSE ratios EB/MLE and EB/VBEM were lower than 10% at $K = K^*$ when $K^* = 10, \dots, 15$. When K^* went bigger, such as $K^* = 17, 18$ in the simulation, the \tilde{K} for most of the graphs was less than K^* , and the MSE ratios reached a minimum level at some $K < K^*$, which was slightly above 50%.

Table 1 presents the model selection results on the simulated dense graphs from model 1, where we define E_{K^*} and $E_{\tilde{K}}$ as the average deviation of the selected number of blocks \hat{K} from K^* and from \tilde{K} respectively, i.e.

$$E_{K^*} = \frac{1}{M} \sum_{t=1}^M |\hat{K}_t - K^*|, \quad E_{\tilde{K}} = \frac{1}{M} \sum_{t=1}^M |\hat{K}_t - \tilde{K}_t|, \quad (23)$$

where $t \in \{1, \dots, M\}$ is the index of the graphs generated under the same Θ^* , \hat{K}_t is the estimated number of clusters by a model selection criterion, and \tilde{K}_t is the \tilde{K} defined by (22) for the t -th graph. When K^* was small, such as $10 \leq K^* \leq 13$, $\mathcal{J}_{\text{VBEM}}$ and \mathcal{J}_{EB} gave the same results, where both accurately selected $\hat{K} = K^*$ as the optimal number of blocks. As K^* increased, \mathcal{J}_{EB} outperformed $\mathcal{J}_{\text{VBEM}}$, and was comparable to $\mathcal{J}_{\text{CVRP}}$ in terms of E_{K^*} . In fact, for a limited graph size $n = 200$ here, the average number of vertices in each block will be smaller as K^* increases, making it hard for small communities to be detected. Therefore, \tilde{K} may better reflect the number of clusters that fit well the observed network. Considering this, we see \mathcal{J}_{EB} had both smaller E_{K^*} and $E_{\tilde{K}}$ than $\mathcal{J}_{\text{VBEM}}$ in general, which indicates the superiority of our model selection method. $\mathcal{J}_{\text{CVRP}}$ showed relatively stable performance in terms of E_{K^*} and $E_{\tilde{K}}$, but the results were not satisfactory for small K^* . In summary, from the simulation results on dense graphs (model 1), EB has demonstrated the highest estimation accuracy,

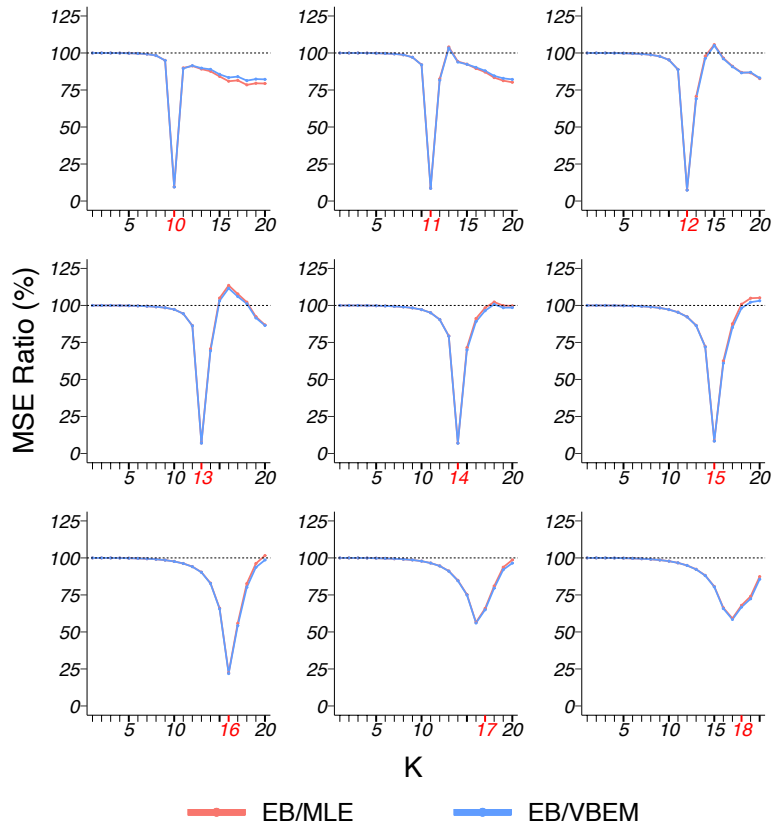


Figure 2 – MSE ratios in model 1 simulation. The true number of blocks K^* (marked in red) ranges from 10 to 18 and the results for graphs with each K^* are shown in a panel. For the 100 graphs generated under each K^* , the MSE ratios of the estimates $\hat{\Theta}_{MLE}$ and $\hat{\Theta}_{VBEM}$ over $\hat{\Theta}_{EB}$ are plotted against the input number of blocks K chosen in the clustering step.

Table 1 – Model selection comparison for model 1 among the \hat{K} chosen by (a) CVRP, (b) VBEM, and (c) EB. (Each row in a table reports the frequency of \hat{K} across 100 graphs. The last two columns report two mean absolute deviations, the minimum of which among the three methods is in boldface for each K^*).

(a) CVRP

$K^* \setminus \hat{K}$	8	9	10	11	12	13	14	15	16	17	18	E_{K^*}	$E_{\hat{K}}$
10		99	1									0.99	0.99
11			100									1.00	1.00
12			3	96	1							1.02	1.02
13					67	33						0.67	0.67
14					6	93		1				1.06	1.06
15						23	77					1.23	1.26
16						2	13	85				1.17	1.31
17							1	29	70			1.31	1.33
18								3	87	10		1.93	1.27

(b) VBEM

$K^* \setminus \hat{K}$	8	9	10	11	12	13	14	15	16	17	18	E_{K^*}	$E_{\hat{K}}$
10			100									0.00	0.00
11				100								0.00	0.00
12					100							0.00	0.00
13						100						0.00	0.00
14						4	96					0.04	0.45
15					1	2	35	62				0.39	0.85
16						1	28	53	18			1.12	1.26
17						6	53	35	6			2.59	2.61
18					1	7	32	44	16			3.33	2.67

(c) EB

$K^* \setminus \hat{K}$	8	9	10	11	12	13	14	15	16	17	18	E_{K^*}	$E_{\hat{K}}$
10			100									0.00	0.00
11				100								0.00	0.00
12					100							0.00	0.00
13						100						0.00	0.00
14							100					0.00	0.00
15							1	99				0.01	0.04
16								30	70			0.30	0.44
17								33	67			1.33	1.35
18								1	95	4		1.97	1.31

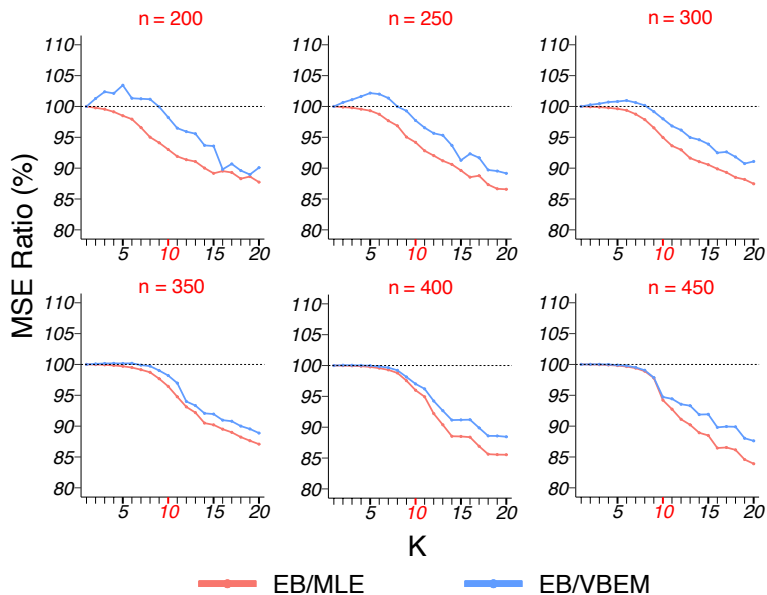


Figure 3 – MSE ratios in model 2 simulation. The results for graphs with each network size n are shown in a panel, plotted in the same format as Figure 2.

especially when the clustering algorithm finds the true number of communities, and the EB model selection criterion generally selects the best model.

Detecting the true number of blocks for a sparse graph (model 2) is harder because of fewer edge connections in a block. Thus, we fixed $K^* = 10$ and varied the network size n from 200 to 450. In terms of estimation accuracy, Figure 3 shows that our EB estimate had better performance than MLE in almost all the cases (except when $K = 1$ under which the two estimates were identical), and the MSE ratio kept decreasing as K increased. In particular, for $K = K^* = 10$, the MSE ratio of EB over MLE was about 95%. If the number of blocks is overestimated (say $K > 15$), the MSE ratio can drop to $< 90\%$. When compared to VBEM, for a small network size n and a small number of blocks K , EB estimates can be slightly less accurate ($< 5\%$ increase in MSE), but as K increases and becomes close to K^* , the MSE ratio goes down to the same level as that of EB over MLE. As reported in Table 2, for all the cases \mathcal{J}_{EB} achieved the best model selection performance with the smallest E_{K^*} and $E_{\tilde{K}}$ among the three methods. This highlights the usefulness of our model selection criterion for the more challenging sparse graph settings.

More detailed results for both models 1 and 2 in this simulation study can be found in Section S1.2 in the Supplementary Material.

Table 2 – Model selection comparison for model 2 among the \hat{K} chosen by (a) CVRP, (b) VBEM, and (c) EB, in similar format as Table 1.

(a) CVRP

$n \setminus \hat{K}$	1	2	3	4	5	6	7	8	9	10	11	12	E_{K^*}	$E_{\hat{K}}$
200	100												9	2.84
250	100												9	6.86
300	95								1	4			8.56	8.84
350	71							1	14	14			6.55	8.17
400	37								28	35			3.61	5.21
450	17								11	71	1		1.65	2.50

(b) VBEM

$n \setminus \hat{K}$	1	2	3	4	5	6	7	8	9	10	11	12	E_{K^*}	$E_{\hat{K}}$
200	28	51	19	2									8.05	2.18
250		8	30	42	13	6			1				6.16	4.04
300			1	11	31	37	20						4.36	4.59
350						14	43	36	7				2.64	4.22
400							3	34	47	14	1	1	1.27	2.83
450							1	3	37	52	6	1	0.54	1.25

(c) EB

$n \setminus \hat{K}$	1	2	3	4	5	6	7	8	9	10	11	12	E_{K^*}	$E_{\hat{K}}$
200		6	12	24	29	24	4	1					5.31	2.09
250				6	21	38	21	12	2				3.82	2.20
300					1	13	32	35	18	1			2.41	2.74
350							2	31	47	20			1.15	2.81
400								10	38	48	3	1	0.63	2.13
450								2	13	78	7		0.24	0.97

3.2. Results on graphon models

Following the same design as in [Latouche and Robin \(2016\)](#), we choose a graphon function

$$W(x, y) = \rho\lambda^2(xy)^{\lambda-1}$$

with two parameters $\lambda \leq 1/\sqrt{\rho}$. Here, ρ controls the sparsity of the graph, as the expected number of edges is proportional to ρ , and λ controls the concentration of the degrees, so that more edges will concentrate on fewer nodes if λ is large. We chose $\rho \in \{10^{-1}, 10^{-1.5}, 10^{-2}\}$ and $\lambda \in \{2, 3, 5\}$, and simulated graphs of size $n = 100$ (model 3) and of size $n = 316$ ($\approx 10^{2.5}$) (model 4). For each network, we used SBM approximation (Section 2.3) with the number of clusters $K = 1, 2, \dots, 10$. Using (22), we also defined \tilde{K} as the number of blocks that minimizes the MSE (19) of the MLE.

The MSE ratios between our EB estimate and the other two competing methods, MLE and VBEM, are shown in Figure 4 for graphs of size $n = 100$ and Figure 5 for graphs of size $n = 316$. In general, our EB method achieved higher accuracy with smaller MSEs than the other two methods. For most cases, our EB estimate was more accurate than the MLE, with the MSE ratios between 60% and 100%. Compared to VBEM, our EB estimate achieved substantially smaller MSEs with ratios below 20%. For both graph sizes, the improvement of the EB method over the other two competitors was especially significant when the graph was sparse (ρ small).

The model selection results are reported in Table 3. Since the true number of communities under the graphon model is not clearly defined, we used \tilde{K} as the ground-truth to evaluate model selection performance. For both $n = 100$ and $n = 316$, the mean absolute deviation $E_{\tilde{K}}$ (23) of the \hat{K} selected by our criterion \mathcal{J}_{EB} was either the smallest or was very close to the smallest value among the three methods. While EB and VBEM were generally comparable, CVRP showed unstable performance as its $E_{\tilde{K}}$ could be much larger than the other two methods in some cases (such as $\rho = 10^{-1}$ and $\rho = 10^{-1.5}$). See Section S1.2 in the Supplementary Material for more detailed results.

We briefly summarize a few key observations from the simulation studies. It is seen that EB estimates had smaller MSEs than the other two methods in most of the cases above. For the dense SBM (model 1), the accuracy of EB estimate was much higher. The relative low variance in connectivity across different blocks led to higher degree of shrinkage and information sharing among the EB estimates. For the sparse SBM (model 2) and graphon models (model 3 and 4), EB showed moderate improvements over the two competing methods in general. When the graph is sparse, EB can be much more accurate than VBEM, as shown in Figures 4 and 5. As for model selection, EB generally selected the number of clusters \hat{K} that was closer to K^* and \tilde{K} in all the models above, which demonstrates the

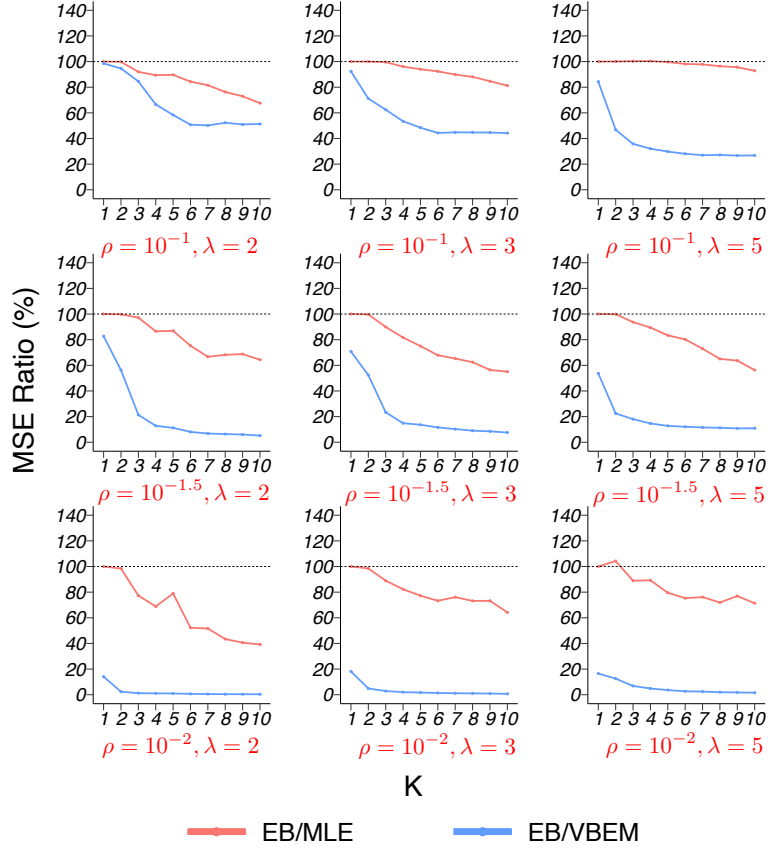


Figure 4 – MSE ratios in model 3 simulation with graph size $n = 100$. The results for graphs with each combination of ρ and λ are shown in a panel.

Table 3 – Model selection comparison for graphons. (Reported is the mean absolute deviation $E_{\tilde{K}}$ for graphs generated under each combination of (ρ, λ) . The minimal $E_{\tilde{K}}$ among the three methods is highlighted in boldface.)

		$n = 100$			$n = 316$		
		CVRP	VBEM	EB	CVRP	VBEM	EB
$\rho = 10^{-1}$	$\lambda = 2$	1.16	0.96	1.11	4.92	2.55	2.38
	$\lambda = 3$	5.42	1.54	2.03	5.8	1.92	1.91
	$\lambda = 5$	3.88	1.28	1.63	7.43	1.66	1.50
$\rho = 10^{-1.5}$	$\lambda = 2$	2.01	1.86	1.83	4.76	3.72	3.70
	$\lambda = 3$	1.81	1.02	0.95	3.93	2.02	1.96
	$\lambda = 5$	2.05	1.03	0.98	4.58	1.60	1.79
$\rho = 10^{-2}$	$\lambda = 2$	0.86	0.85	0.86	2.56	2.24	2.25
	$\lambda = 3$	1.41	1.45	1.48	1.48	1.35	1.31
	$\lambda = 5$	1.52	1.61	1.7	2.77	1.72	1.67

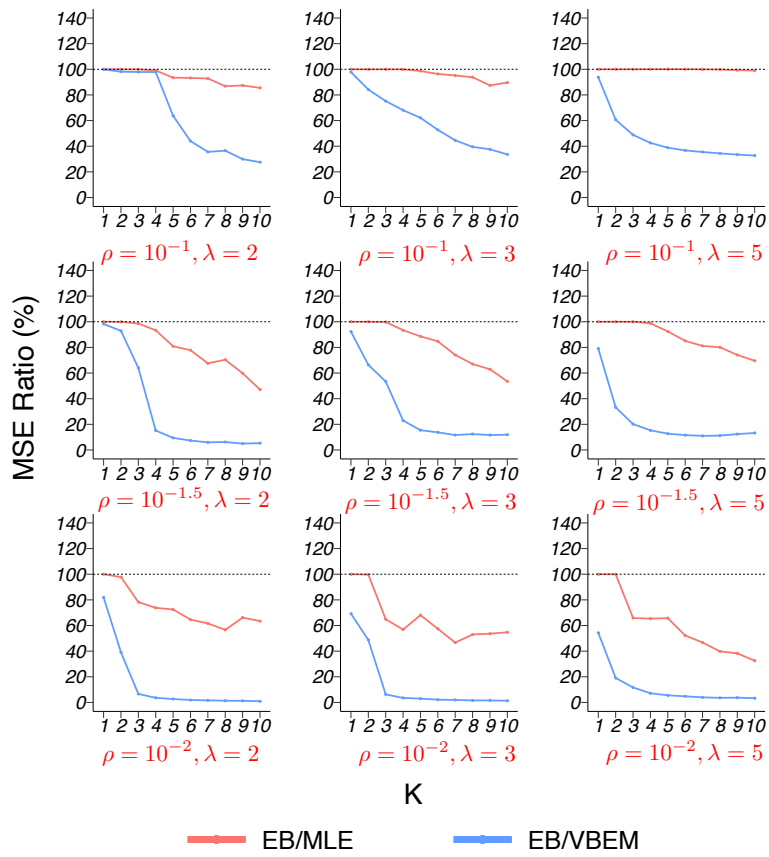


Figure 5 – MSE ratios in model 4 simulation with graph size $n = 316$. The results for graphs with each combination of ρ and λ are shown in a panel.

usefulness of our hierarchical model for deriving likelihood-based model selection criterion.

3.3. Alternative clustering and complexity

Our results and numerical comparisons in Section 3.1 and 3.2 were conducted to demonstrate the uniform accuracy improvement: By varying the input number of clusters so some cluster results could be very inaccurate, our EB estimates reached smaller MSEs for almost all the clustering results. To further demonstrate this point, we also applied our EB estimates after spectral clustering. As shown in Figure 6, our method improved the parameter estimation accuracy as well: Under the same setting as in Figure 2 and Figure 3. The EB/MLE MSE ratio shows a similar pattern to the results of the previous simulation in SBM for both cases.

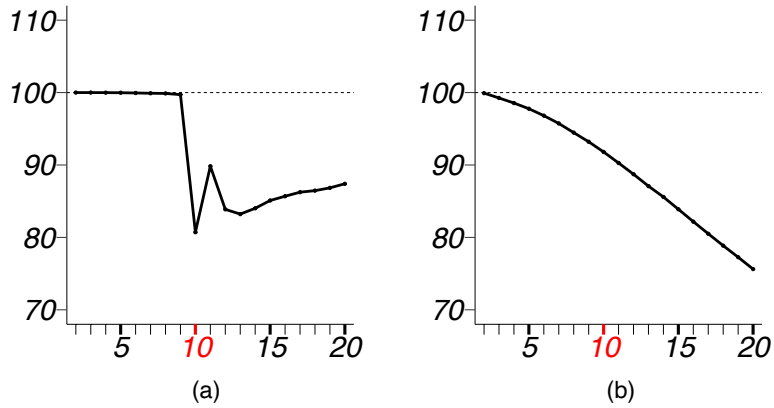


Figure 6 – MSE ratios in spectral clustering simulation. (a) model 1 with parameters $K^* = 10$, $n = 200$. (b) model 2 with parameters $K^* = 10$, $n = 450$.

The computation of our EB method is only the maximization of the likelihood (8, 9). The objective is the sum of two separate functions. Thus, we just need to maximize two bi-variate functions, regardless of the problem size (n, K) . In general, the computation time is negligible compared to the graph clustering step. Table 4 reports the average running times (in seconds) of spectral clustering (T_C) and our EB estimation (T_E) by BFGS for various network size n and number of communities K , on a single 2.6 GHz Intel i7 core.

4. Real Data Examples

In this section, we apply our empirical Bayes method on two real-world networks. For real-world networks, we do not have the underlying connectivity

Table 4 – Simulation running time.

(n, K)	(100, 10)	(1000, 10)	(1000, 100)	(5000, 10)	(5000, 100)	(10000, 500)
T_C	0.06	0.7	4.4	6.7	149	2696
T_E	0.08	0.1	0.2	0.6	1.9	11.6

matrix as the ground truth, which makes it difficult to evaluate estimation accuracy. However, for a network with known node labels that indicate their community memberships (the “ground truth”), the true partition Z_{true} of the vertices is given. Thus, we will develop accuracy metrics based on Z_{true} to compare different methods.

4.1. Email-Eu-core network

The Email-Eu-core network (Eucore) is a directed network generated using email data from a large European institute, consisting of incoming and outgoing communications between members of the institute from 42 departments. Leskovec and Krevl (2014) organized the data and labeled which department each individual node belongs to, i.e. the “ground-truth” community memberships. The network has $n = 1005$ nodes and 25,571 directed edges, which we converted to undirected ones by removing their orientations. We applied VBEM to detect communities with an input number of clusters $K = 30, 31, \dots, 50$.

Given the known community memberships, we constructed a connectivity matrix $\Theta^* = (\theta_{ab}^*)_{K^* \times K^*}$ with entries

$$\theta_{ab}^* = X_{ab}^B / n_{ab}, \quad a, b \in \{1, \dots, K^*\}, \quad (24)$$

where X_{ab}^B is the number of edges observed in block (a, b) , $n_{ab} = |Z_{\text{true}}^{-1}(a)| \cdot |Z_{\text{true}}^{-1}(b)|$ for $a \neq b$ and $n_{aa} = |Z_{\text{true}}^{-1}(a)| \cdot (|Z_{\text{true}}^{-1}(a)| - 1)/2$, and K^* is the true number of communities. Then the MSE (18) between an estimate $\hat{\Theta}(K)$ and Θ^* (24) were used as an accuracy metric to compare estimated connectivity matrices, where K is the input number of clusters.

We also used test data likelihood as another comparison metric. We randomly sampled 70% of the nodes, denoted by V_o , as observed training data, and estimated a connectivity matrix $\hat{\Theta} = (\hat{\theta}_{ij})_{K^* \times K^*}$ from their edge connections and true memberships. Denote by V_t the test data nodes not used in the estimation. Recall that X_{ij} is the (i, j) th element in the adjacency matrix of the network. Then test data likelihood $\mathcal{L}_{\text{test}}$ was calculated according to (2) given the $\hat{\Theta}$ estimated by a method,

$$\mathcal{L}_{\text{test}} = \prod_{i \in V_o, j \in V_t} \hat{\theta}_{z_i z_j}^{X_{ij}} (1 - \hat{\theta}_{z_i z_j})^{1 - X_{ij}} \times \prod_{k < j \in V_t} \hat{\theta}_{z_j z_k}^{X_{jk}} (1 - \hat{\theta}_{z_j z_k})^{1 - X_{jk}}, \quad (25)$$

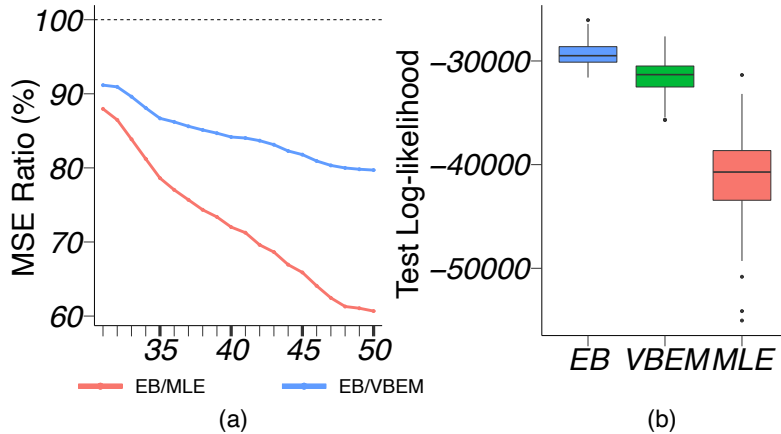


Figure 7 – Results for Email-Eu-core network analysis. (a) The ratio of MSE of EB estimate over that of MLE and VBEM for different values of K . (b) Box-plot of 100 test data log-likelihood values for each method.

where z_i, z_j, z_k are the known labels of the nodes. Note that $X_{ij} \in \{0, 1\}$ is the edge connection between a vertex i in the training data and a vertex j in the test data, while X_{jk} is the edge connection between two vertices j and k in the test data. We repeated this procedure 100 times independently to find the distribution of test data likelihood $\mathcal{L}_{\text{test}}$ across random sample splitting of the n nodes into V_o and V_t .

The MSE ratios of EB over the other two competing methods were calculated and plotted against K in Figure 7(a). It is clear that EB achieved smaller MSE than the other two methods for all values of K . The MSE ratios ranged from 60% to 90%. When the input number of communities K was close to or greater than $K^* = 42$, the improvement of EB over the competing methods became more substantial. Figure 7(b) shows the box-plot of test data log-likelihood values across 100 random sample splitting. From the box-plots, we see that the test data likelihood of EB was significantly higher than the other two estimates. These comparisons confirm that EB estimates were more accurate than the other two competing methods in terms of both metrics.

We further applied the three model selection methods, CVRP, VBEM and EB, on the whole network, and they gave estimates $\hat{K} = 31, 43$ and 37 , respectively. The \hat{K} by VBEM and EB were both reasonably close to the ground-truth of $K^* = 42$.

4.2. Political Blogs

Next we consider the French political blogosphere network from [Latouche et al. \(2011\)](#). The network is made of 196 vertices connected by 2864 edges. It

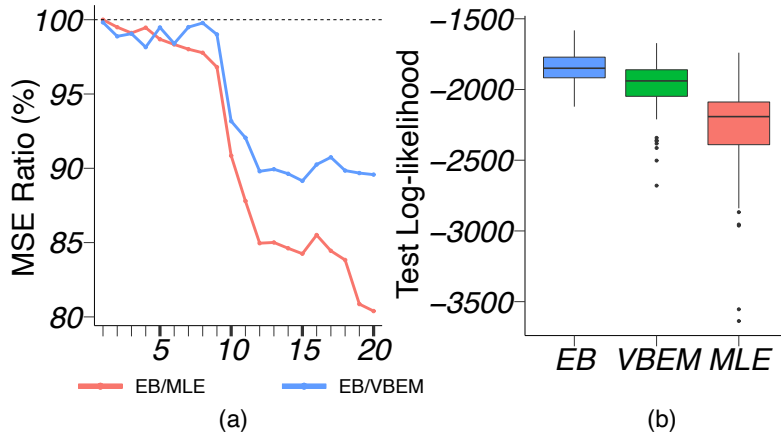


Figure 8 – Results for French blogosphere network analysis in the same format as Figure 7.

was built from a single day snapshot of political blogs automatically extracted on October 14th, 2006 and manually classified by the “Observatoire Presidentiel” project (Zanghi et al. 2008). In this network, nodes correspond to hostnames and there is an edge between two nodes if there is a known hyperlink from one hostname to the other. The four main political parties that are present in the data set are the UMP (french republican), liberal party (supporters of economic-liberalism), UDF (moderate party), and PS (french democrat). However, in the dataset annotated by Latouche et al. (2011) there are $K^* = 11$ different node labels in total, since they considered analysts as well as subgroups of the parties.

We applied the same analyses as in Section 4.1 with input $K = 1, \dots, 20$. The MSE and test data likelihood results are shown in Figure 8. When K was close to or greater than $K^* = 11$, EB provided more accurate estimates than both MLE and VBEM with smaller MSEs. Similarly, the box-plots in Figure 8(b) demonstrate that the test data log-likelihood calculated with EB estimates was significantly higher than the two competing methods. In terms of model selection, CVRP, VBEM and EB estimated $\hat{K} = 1, 12$ and 10 respectively, while the true $K^* = 11$. Again, the latter two criteria worked quite well on this network.

5. Discussion

In this paper, we developed an empirical Bayes estimate for the probabilities of edge connections between communities in a network. While empirical Bayes (EB) under a hierarchical model is a well-established method, its application to SBMs is very limited before our work. Our method is a natural fit to the SBM and the idea is generally applicable to different community detection methods. It does not require complicated algorithms or heavy computation, yet can effectively improve

the estimation accuracy of model parameters. For the large volume of published community detection or network clustering algorithms, our parameter estimation method can be adopted as a superior alternate after the node clustering step. SBM approximation to graphons could result in a large number of blocks, for which case the EB often shows substantial advantage over the MLE, and this was a key motivation for our generalization to graphon estimation. This also helps the development of a good model selection criterion based on the marginal likelihood.

Though shrinkage in empirical Bayes approach leads to more accurate estimate of the connectivity probabilities, the improvement depends on the variability of the underlying connectivity matrix or graphon function. Typically, a higher variance reduces its improvement relative to the MLE. Therefore, for some graphon functions with high volatility, EB cannot guarantee a better estimate, but from our simulation results, EB estimate and MLE are usually comparable for such cases. A main reason for this observation is that EB estimate uses a very small number of hyperparameters, which effectively reduces the model complexity via shrinkage and greatly minimizes the risk of overfitting the data.

5.1. Future works

We put a beta conjugate prior on connection probability Θ , and the estimates of the hyperparameters $(\alpha_d, \beta_d)_{d=\{0,1\}}$ will not be 0. Thus when there is a true connectivity $\theta_{ab} = 0$ in block (a, b) , which is likely to happen in sparse networks, our hierarchical model introduces bias to the estimate of θ_{ab} . However, since the empirical Bayes estimator is pooling data in all the blocks, the overall accuracy should still be higher. To alleviate this biased fitting problem, we can build the likelihood only on blocks with observed connections, or consider adding only a proportion α of zero connectivity blocks. This method can be tested with more experiments to find out which α works the best under different assumptions of SBM and graphon.

In our experiments, we compared the model estimation accuracy by their mean squared error, which is a gold standard criterion to evaluate parameter estimation. However several other metrics such as KL-divergence of the estimated graphon function to the truth, deviation of the estimated number of motifs in the graph to the true value, and divergence of degree distributions can also be considered. For the application on real data, the goodness of fit of SBM or graphon model to the dataset should be checked by comparison to other existing network modeling methods. A decent fit of the stochastic blockmodel and graphon to the chosen dataset will strengthen the persuasiveness of the usefulness of our method.

We have focused on parameter estimation for binary and assortative stochastic block models and graphons. In fact, this idea can be generalized to more sophisticated random graph models, such as SBM with mixed memberships (Airoldi

et al. 2008), SBM with weighted edges (Aicher et al. 2015), and bipartite SBM (Larremore et al. 2014) etc. While most of the related works focus on graph clustering, our empirical Bayes method can be applied after clustering to improve the estimation accuracy and to identify a proper number of blocks for these models.

Acknowledgement

This work was supported in part by NSF grant DMS-1952929.

References

- Réka Albert and Albert-László Barabási. Statistical mechanics of complex networks. *Reviews of Modern Physics*, 74(1):47–97, Jan 2002.
- Albert-László Barabási and Réka Albert. Emergence of scaling in random networks. *Science*, 286(5439):509–512, 1999.
- M. E. J. Newman, D. J. Watts, and S. H. Strogatz. Random graph models of social networks. *Proceedings of the National Academy of Sciences*, 99(suppl 1):2566–2572, 2002.
- M. Girvan and M. E. J. Newman. Community structure in social and biological networks. *Proceedings of the National Academy of Sciences*, 99(12):7821–7826, 2002.
- M. E. J. Newman. Fast algorithm for detecting community structure in networks. *Physical Review E*, 69(6), Jun 2004.
- Linton C. Freeman. Spheres, cubes and boxes: Graph dimensionality and network structure. *Social Networks*, 5(2):139 – 156, 1983.
- James Lloyd, Peter Orbanz, Zoubin Ghahramani, and Daniel M Roy. Random function priors for exchangeable arrays with applications to graphs and relational data. In F. Pereira, C. J. C. Burges, L. Bottou, and K. Q. Weinberger, editors, *Advances in Neural Information Processing Systems 25*, pages 998–1006. Curran Associates, Inc., 2012.
- Laszlo Lovasz and Balazs Szegedy. Limits of dense graph sequences. *Journal of Combinatorial Theory, Series B*, 96(6):933 – 957, 2006.
- Emmanuel Abbe. Community detection and stochastic block models: Recent developments. *Journal of Machine Learning Research*, 18(177):1–86, 2018.
- Krzysztof Nowicki and Tom A. B Snijders. Estimation and prediction for stochastic blockstructures. *Journal of the American Statistical Association*, 96(455):1077–1087, 2001.
- Antoine Channarond, Jean-Jacques Daudin, and Stéphane Robin. Classification and estimation in the stochastic blockmodel based on the empirical degrees. *Electron. J. Statist.*, 6:2574–2601, 2012.
- J.-J. Daudin, F. Picard, and S. Robin. A mixture model for random graphs. *Statistics and Computing*, 18(2):173–183, Jun 2008.
- P Latouche, E Birmele, and C Ambroise. Variational bayesian inference and complexity control for stochastic block models. *Statistical Modelling*, 12(1):93–115, 2012.
- Shakira Suwan, Dominic S. Lee, Runze Tang, Daniel L. Sussman, Minh Tang, and Carey E. Priebe. Empirical bayes estimation for the stochastic blockmodel. *Electron. J. Statist.*, 10(1):761–782, 2016.
- Stephen J. Young and Edward R. Scheinerman. Random dot product graph models for social networks. In *Algorithms and Models for the Web-Graph*, pages 138–149. Springer Berlin Heidelberg, 2007.
- Edo M Airoldi, Thiago B Costa, and Stanley H Chan. Stochastic blockmodel approximation of a graphon: Theory and consistent estimation. In C. J. C. Burges, L. Bottou, M. Welling, Z. Ghahramani, and K. Q. Weinberger, editors, *Advances in Neural Information Processing Systems 26*, pages 692–700. Curran Associates, Inc., 2013.
- Sofia C. Olhede and Patrick J. Wolfe. Network histograms and universality of blockmodel approximation. *Proceedings of the National Academy of Sciences*, 111(41):14722–14727, 2014.
- Pierre Latouche and Stéphane Robin. Variational bayes model averaging for graphon functions and motif frequencies inference in w-graph models. *Statistics and Computing*, 26(6):1173–1185, Nov 2016.
- Bradley Efron. *Large-Scale Inference: Empirical Bayes Methods for Estimation, Testing, and Prediction*. Institute of Mathematical Statistics Monographs. Cambridge University Press, 2010.
- Karl Rohe, Sourav Chatterjee, and Bin Yu. Spectral clustering and the high-dimensional stochastic blockmodel. *Ann. Statist.*, 39(4):1878–1915, 08 2011.

- Leon Danon, Albert Díaz-Guilera, Jordi Duch, and Alex Arenas. Comparing community structure identification. *Journal of Statistical Mechanics: Theory and Experiment*, 2005(09): P09008–P09008, Sep 2005.
- Richard H. Byrd, Peihuang Lu, Jorge Nocedal, and Ciyou Zhu. A limited memory algorithm for bound constrained optimization. *SIAM Journal of Scientific Computing*, 16:1190–1208, 9 1995.
- Harold Jeffreys. An invariant form for the prior probability in estimation problems. *Proceedings of the Royal Society of London. Series A. Mathematical and Physical Sciences*, 186(1007): 453–461, 1946.
- Mahendra Mariadassou, Stéphane Robin, and Corinne Vacher. Uncovering latent structure in valued graphs: A variational approach. *Ann. Appl. Stat.*, 4(2):715–742, 06 2010.
- Peter J. Bickel and Aiyu Chen. A nonparametric view of network models and newman–girvan and other modularities. *Proceedings of the National Academy of Sciences*, 106(50):21068–21073, 2009.
- Jure Leskovec and Andrej Krevl. SNAP Datasets: Stanford large network dataset collection, jun 2014.
- Pierre Latouche, Etienne Birmelé, and Christophe Ambroise. Overlapping stochastic block models with application to the french political blogosphere. *The Annals of Applied Statistics*, 5(1):309–336, Mar 2011.
- Hugo Zanghi, Christophe Ambroise, and Vincent Miele. Fast online graph clustering via erdős–rényi mixture. *Pattern Recognition*, 41(12):3592 – 3599, 2008.
- Edoardo M. Airoldi, David M. Blei, Stephen E. Fienberg, and Eric P. Xing. Mixed membership stochastic blockmodels. *J. Mach. Learn. Res.*, 9:1981–2014, June 2008.
- Christopher Aicher, Abigail Z. Jacobs, and Aaron Clauset. Learning latent block structure in weighted networks. *J. Complex Networks*, 3:221–248, 2015.
- Daniel B. Larremore, Aaron Clauset, and Abigail Z. Jacobs. Efficiently inferring community structure in bipartite networks. *Phys. Rev. E*, 90:012805, Jul 2014.
- M.J. Beal and Z. Ghahramani. The variational bayesian em algorithm for incomplete data : with application to scoring graphical model structures. *Bayesian Statistics*, 7:453–464, 2003.

S1. Supplementary Material

S1.1. Variational Bayes EM algorithm

As an extension to the work in [Daudin et al. \(2008\)](#), [Latouche et al. \(2012\)](#) proposed a variational Bayes approximation to provide a closed form approximate posterior distribution of the parameters (π, Θ) and of the latent variables \mathbf{Z} , where the observed-data log-likelihood can be decomposed into two terms,

$$\ln p(\mathbf{X}) = \mathcal{L}(q(\cdot)) + \text{KL}(q(\cdot) \| p(\cdot | \mathbf{X})), \quad (26)$$

where

$$\mathcal{L}(q(\cdot)) = \sum_{\mathbf{Z}} \int \int q(\mathbf{Z}, \pi, \Theta) \ln \left\{ \frac{p(\mathbf{X}, \mathbf{Z}, \pi, \Theta)}{q(\mathbf{Z}, \pi, \Theta)} \right\} d\pi d\Theta, \quad (27)$$

and

$$\text{KL}(q(\cdot) \| p(\cdot | \mathbf{X})) = - \sum_{\mathbf{Z}} \int \int q(\mathbf{Z}, \pi, \Theta) \ln \left\{ \frac{p(\mathbf{Z}, \pi, \Theta | \mathbf{X})}{q(\mathbf{Z}, \pi, \Theta)} \right\} d\pi d\Theta. \quad (28)$$

Minimizing (28) with respect to $q(\mathbf{Z}, \pi, \Theta)$ is equivalent to maximizing the lower bound (27) with respect to $q(\mathbf{Z}, \pi, \Theta)$. However, when considering SBM, $q(\mathbf{Z}, \pi, \Theta)$ is intractable, thus we can assume that it can be factorized as

$$q(\mathbf{Z}, \pi, \Theta) = q(\mathbf{Z})q(\pi)q(\Theta) = q(\pi)q(\Theta) \prod_{i=1}^N q(z_i), \quad (29)$$

where the optimal approximation $q(z_i)$ at vertex i follows a multinomial distribution. [Latouche et al. \(2012\)](#) used a variational Bayes EM (VBEM) algorithm described in [Beal and Ghahramani \(2003\)](#) to optimize over $q(z_i)$ and $q(\pi)$, $q(\Theta)$ iteratively.

S1.2. Supplementary figures and tables

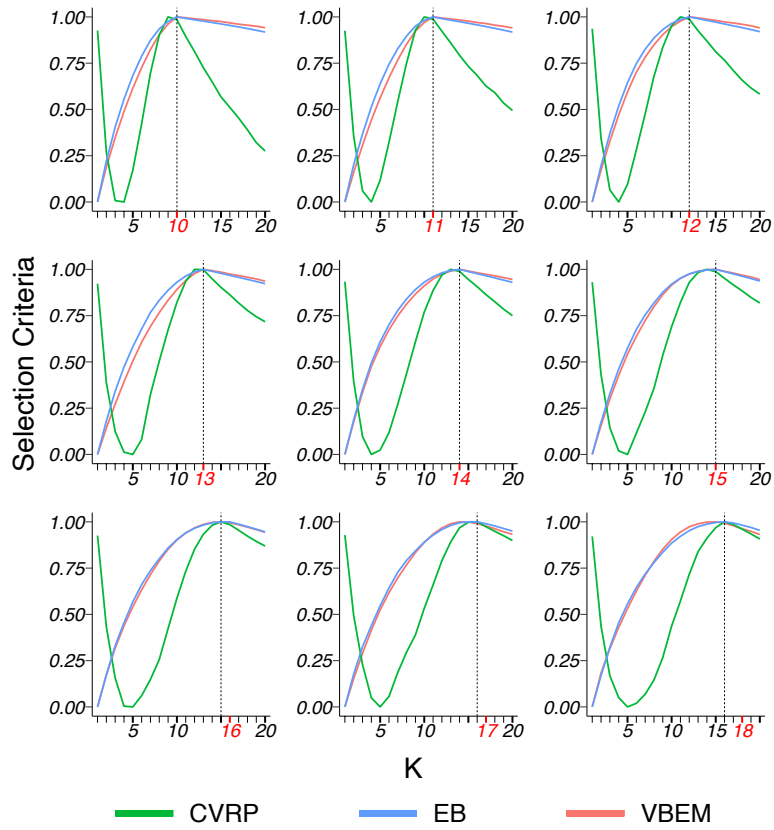


Figure S1 – Values of model selection criteria in model 1 simulation. The true number of blocks K^* (marked as red) ranges from 10 to 18 and the results for graphs with each K^* are shown in a panel. $\mathcal{J}_{\text{CVRP}}$, $\mathcal{J}_{\text{VBEM}}$, \mathcal{J}_{EB} are all standardized to $[0, 1]$, and $\mathcal{J}_{\text{CVRP}}$ is taken negative, thus the model is selected by the maximizer of each criterion. For the 100 graphs generated under each set of parameters, the values of three criteria are plotted against the input number of blocks $K = 1, \dots, 20$ used in clustering. The number of clusters selected by EB is highlighted by the dashed lines.

Table S1 – MSE values for model 1. The average MSE of the estimates $\hat{\Theta}$ to Θ by the three methods of the 100 graphs generated under different K^* are shown in each row. The input number of clusters K ranges from 10 to 18, for each K^* and K the minimal MSE among three methods is boldfaced.

$K^* \setminus K$	9	10	11	12	13	14	15	16	17	18	19	20		
10	MLE	304	25	35	46	56	67	77	93	109	120	131	148	$\times 10^{-5}$
	VBEM	304	25	36	46	55	66	76	90	106	116	127	143	$\times 10^{-5}$
	EB	289	2	32	42	50	59	65	75	89	94	105	117	$\times 10^{-5}$
11	MLE	538	249	30	41	52	60	72	85	96	112	123	139	$\times 10^{-5}$
	VBEM	538	249	31	41	52	60	72	85	95	111	120	136	$\times 10^{-5}$
	EB	522	229	3	34	54	56	66	76	83	94	100	111	$\times 10^{-5}$
12	MLE	683	417	215	35	44	55	67	79	89	99	112	130	$\times 10^{-5}$
	VBEM	683	417	216	36	45	56	67	79	89	100	112	129	$\times 10^{-5}$
	EB	668	398	192	3	31	54	70	76	81	86	97	107	$\times 10^{-5}$
13	MLE	1012	708	434	212	41	51	62	75	85	98	111	128	$\times 10^{-5}$
	VBEM	1012	708	434	212	42	52	63	76	86	99	112	128	$\times 10^{-5}$
	EB	996	689	410	183	3	36	65	85	91	100	103	111	$\times 10^{-5}$
14	MLE	921	692	487	305	167	48	60	71	81	91	102	114	$\times 10^{-5}$
	VBEM	921	692	488	305	168	49	61	73	82	93	104	116	$\times 10^{-5}$
	EB	906	673	464	276	133	3	43	65	79	94	102	114	$\times 10^{-5}$
15	MLE	969	733	543	389	262	149	57	68	78	88	99	114	$\times 10^{-5}$
	VBEM	969	733	543	390	263	150	58	70	81	91	102	116	$\times 10^{-5}$
	EB	953	712	518	359	227	108	5	43	69	89	104	120	$\times 10^{-5}$
16	MLE	1044	842	653	495	361	237	137	70	77	89	101	114	$\times 10^{-5}$
	VBEM	1044	842	653	495	362	238	138	72	80	92	104	117	$\times 10^{-5}$
	EB	1028	822	629	466	326	197	91	16	43	74	97	115	$\times 10^{-5}$
17	MLE	1132	907	705	541	388	264	190	124	124	125	137	146	$\times 10^{-5}$
	VBEM	1132	907	705	541	389	265	191	125	126	128	140	149	$\times 10^{-5}$
	EB	1116	887	681	512	354	224	143	70	82	102	129	144	$\times 10^{-5}$
18	MLE	1097	905	733	583	458	348	247	161	137	142	141	164	$\times 10^{-5}$
	VBEM	1097	905	733	583	458	348	248	162	139	144	144	167	$\times 10^{-5}$
	EB	1082	886	709	553	423	307	199	107	81	96	104	143	$\times 10^{-5}$

Table S2 – MSE values for model 2. The average MSE of the estimates $\hat{\Theta}$ to Θ by the three methods of the 100 graphs generated under different n are shown in each row. The input number of clusters K ranges from 1 to 12, for each n and K the minimal MSE among three methods is boldfaced.

$n \setminus K$	1	2	3	4	5	6	7	8	9	10	11	12		
200	MLE	229	225	225	229	236	238	247	256	266	269	273	283	$\times 10^{-5}$
	VBEM	229	221	219	222	225	230	236	240	251	255	260	269	$\times 10^{-5}$
	EB	229	224	224	227	233	233	239	243	250	250	251	258	$\times 10^{-5}$
250	MLE	230	217	204	192	186	182	184	187	192	193	202	206	$\times 10^{-5}$
	VBEM	230	215	201	188	181	176	177	181	184	186	194	198	$\times 10^{-5}$
	EB	230	217	203	192	185	180	180	181	182	182	187	190	$\times 10^{-5}$
300	MLE	231	208	186	165	147	130	121	120	118	124	128	133	$\times 10^{-5}$
	VBEM	231	208	185	164	145	128	119	117	114	120	123	128	$\times 10^{-5}$
	EB	231	208	186	165	147	130	120	117	113	117	119	123	$\times 10^{-5}$
350	MLE	231	202	175	151	129	110	94	81	74	75	77	77	$\times 10^{-5}$
	VBEM	231	202	174	150	128	109	93	80	73	73	76	76	$\times 10^{-5}$
	EB	231	202	175	150	128	110	93	80	73	72	73	72	$\times 10^{-5}$
400	MLE	232	201	171	141	117	95	77	61	49	44	43	45	$\times 10^{-5}$
	VBEM	232	201	170	141	117	95	77	60	48	44	42	44	$\times 10^{-5}$
	EB	232	201	170	141	117	94	77	60	47	43	41	42	$\times 10^{-5}$
450	MLE	232	199	167	139	114	91	70	52	36	25	26	28	$\times 10^{-5}$
	VBEM	232	199	167	139	114	91	70	52	36	25	26	27	$\times 10^{-5}$
	EB	232	199	167	139	114	91	70	51	35	24	24	26	$\times 10^{-5}$

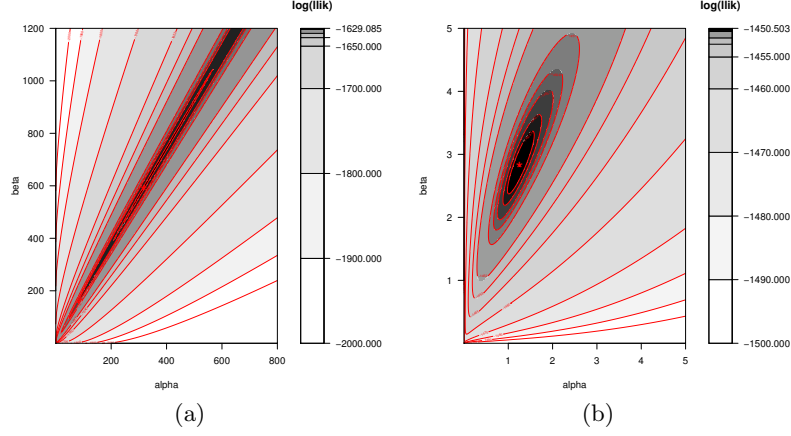


Figure S2 – A typical contour plot of (a) $\mathcal{L}(\alpha_0, \beta_0)$ and (b) $\mathcal{L}(\alpha_1, \beta_1)$ from a graph generated by a SBM with $n = 200$, $K = 5$, $\theta_{ab} = 0.7$ for $a = b$ and $\theta_{ab} = 0.3$ for $a \neq b$. The maximizers are marked as stars in the plots.

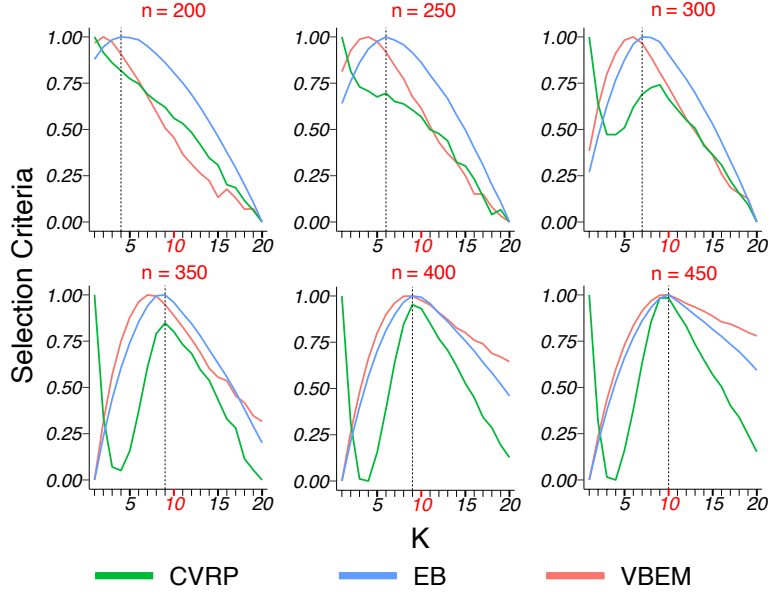


Figure S3 – Values of model selection criteria in model 2 simulation. With the true number of blocks $K^* = 10$ (marked as red), the number of network sizes n ranges from 200 to 450 and the results for graphs with each n are shown in a panel. $\mathcal{J}_{\text{CVRP}}$, $\mathcal{J}_{\text{VBEM}}$, \mathcal{J}_{EB} are all standardized to $[0, 1]$, and $\mathcal{J}_{\text{CVRP}}$ is taken negative, thus the model is selected by the maximizer of each criterion. For the 100 graphs generated under each set of parameters, the values of three criteria are plotted against the input number of blocks $K = 1, \dots, 20$ used in clustering. The number of clusters selected by EB is highlighted by the dashed lines.

Table S3 – MSE values for model 3. The average MSE of the estimates $\hat{\Theta}$ to Θ by the three methods of the 100 graphs generated under different set of parameters ρ and λ are shown in each row. The input number of clusters K ranges from 1 to 10, for each ρ , λ and K the minimal MSE among three methods is boldfaced.

ρ	λ		1	2	3	4	5	6	7	8	9	10		
10^{-1}	2	MLE	80	26	28	34	43	47	57	70	80	91	$\times 10^{-4}$	
		VBEM	81	28	31	46	65	78	92	103	114	120	$\times 10^{-4}$	
		EB	80	26	26	31	38	40	46	54	58	62	$\times 10^{-4}$	
	3	MLE	229	78	47	50	57	62	73	83	94	104	$\times 10^{-4}$	
		VBEM	248	109	75	90	110	130	147	163	177	191	$\times 10^{-4}$	
		EB	229	77	47	48	53	58	66	73	79	84	$\times 10^{-4}$	
	5	MLE	680	247	161	144	144	148	153	164	171	184	$\times 10^{-4}$	
		VBEM	806	529	451	452	483	517	555	581	612	638	$\times 10^{-4}$	
		EB	680	248	161	145	144	145	150	158	163	171	$\times 10^{-4}$	
	$10^{-1.5}$	2	MLE	8	11	13	14	17	18	21	22	24	25	$\times 10^{-4}$
			VBEM	10	20	59	98	133	169	204	234	269	305	$\times 10^{-4}$
			EB	8	11	13	13	15	14	14	15	16	16	$\times 10^{-4}$
3		MLE	23	13	16	19	24	28	32	34	40	42	$\times 10^{-4}$	
		VBEM	32	25	63	102	132	166	202	236	265	304	$\times 10^{-4}$	
		EB	23	13	15	15	18	19	21	21	23	23	$\times 10^{-4}$	
5		MLE	68	30	32	35	40	45	54	64	70	88	$\times 10^{-4}$	
		VBEM	127	132	166	213	258	301	339	369	415	452	$\times 10^{-4}$	
		EB	68	30	30	31	33	36	39	42	45	49	$\times 10^{-4}$	
10^{-2}		2	MLE	82	190	239	336	346	429	425	442	498	490	$\times 10^{-6}$
			VBEM	58	795	1525	2183	2821	3461	4098	4705	5248	5799	$\times 10^{-5}$
			EB	82	187	185	232	273	224	219	192	202	192	$\times 10^{-6}$
	3	MLE	23	44	53	58	68	71	68	73	74	67	$\times 10^{-5}$	
		VBEM	127	889	1644	2397	3103	3814	4509	5164	5774	6413	$\times 10^{-5}$	
		EB	23	43	47	48	53	52	52	53	54	43	$\times 10^{-5}$	
	5	MLE	68	136	153	160	173	165	174	171	160	166	$\times 10^{-5}$	
		VBEM	413	1129	1998	2941	3804	4667	5413	6215	6943	7586	$\times 10^{-5}$	
		EB	68	142	136	143	137	124	132	123	123	118	$\times 10^{-5}$	

Table S4 – MSE values for model 4. The average MSE of the estimates $\hat{\Theta}$ to Θ by the three methods of the 100 graphs generated under different set of parameters ρ and λ are shown in each row. The input number of clusters K ranges from 1 to 10, for each ρ , λ and K the minimal MSE among three methods is boldfaced.

ρ	λ		1	2	3	4	5	6	7	8	9	10		
10^{-1}	2	MLE	782	240	120	77	82	84	87	114	112	121	$\times 10^{-5}$	
		VBEM	783	244	122	78	121	177	228	270	327	374	$\times 10^{-5}$	
		EB	782	240	120	76	77	78	81	99	98	103	$\times 10^{-5}$	
	3	MLE	225	69	33	20	15	14	15	15	18	18	$\times 10^{-4}$	
		VBEM	230	82	44	29	23	26	31	36	42	48	$\times 10^{-4}$	
		EB	225	69	33	20	15	14	14	14	16	16	$\times 10^{-4}$	
	5	MLE	674	230	131	103	91	85	83	83	84	85	$\times 10^{-4}$	
		VBEM	719	379	268	242	234	232	234	241	248	257	$\times 10^{-4}$	
		EB	674	230	131	103	91	85	83	83	83	84	$\times 10^{-4}$	
	$10^{-1.5}$	2	MLE	78	24	21	22	28	32	39	45	52	78	$\times 10^{-5}$
			VBEM	80	26	32	138	242	342	450	512	623	686	$\times 10^{-5}$
			EB	78	24	20	21	23	25	27	32	31	37	$\times 10^{-5}$
3		MLE	225	68	33	37	43	52	65	84	96	125	$\times 10^{-5}$	
		VBEM	244	102	62	151	248	323	416	455	517	559	$\times 10^{-5}$	
		EB	225	68	33	35	38	44	48	56	60	67	$\times 10^{-5}$	
5		MLE	674	213	102	73	79	93	106	119	151	180	$\times 10^{-5}$	
		VBEM	853	641	506	472	577	680	785	854	903	947	$\times 10^{-5}$	
		EB	674	213	102	72	73	79	86	96	112	125	$\times 10^{-5}$	
10^{-2}		2	MLE	8	8	15	15	17	18	20	22	20	18	$\times 10^{-5}$
			VBEM	10	20	176	305	476	626	778	915	1065	1250	$\times 10^{-5}$
			EB	8	8	12	11	13	12	13	12	14	12	$\times 10^{-5}$
	3	MLE	23	9	16	20	21	25	33	29	33	31	$\times 10^{-5}$	
		VBEM	33	19	168	325	471	656	792	994	1121	1301	$\times 10^{-5}$	
		EB	23	9	11	11	14	14	15	15	18	17	$\times 10^{-5}$	
	5	MLE	67	23	35	39	44	60	70	88	105	130	$\times 10^{-5}$	
		VBEM	124	120	196	358	523	655	829	984	1084	1277	$\times 10^{-5}$	
		EB	67	23	23	26	29	31	33	35	40	42	$\times 10^{-5}$	

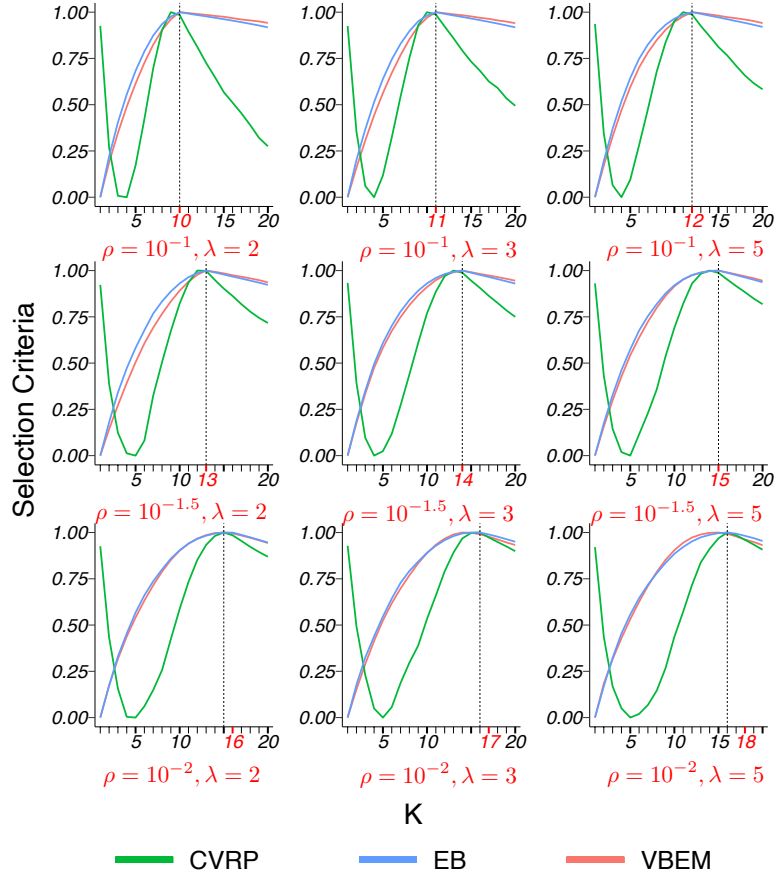


Figure S4 – Values of model selection criteria in model 3 simulation. Graph size (number of nodes) $n = 100$. With the graphon $W(x, y) = \rho\lambda^2(xy)^{\lambda-1}$, $\rho \in \{10^{-1}, 10^{-1.5}, 10^{-2}\}$ and $\lambda \in \{2, 3, 5\}$, the results for graphs with each set of parameters ρ and λ are shown in a panel. $\mathcal{I}_{\text{CVRP}}$, $\mathcal{I}_{\text{VBEM}}$, \mathcal{I}_{EB} are all standardized to $[0, 1]$, and $\mathcal{I}_{\text{CVRP}}$ is taken negative, thus the model is selected by the maximizer of each criterion. For the 100 graphs generated under each set of parameters, the values of three criteria are plotted against the input number of blocks $K = 1, \dots, 10$ used in clustering. The number of clusters selected by EB is highlighted by the dashed lines.

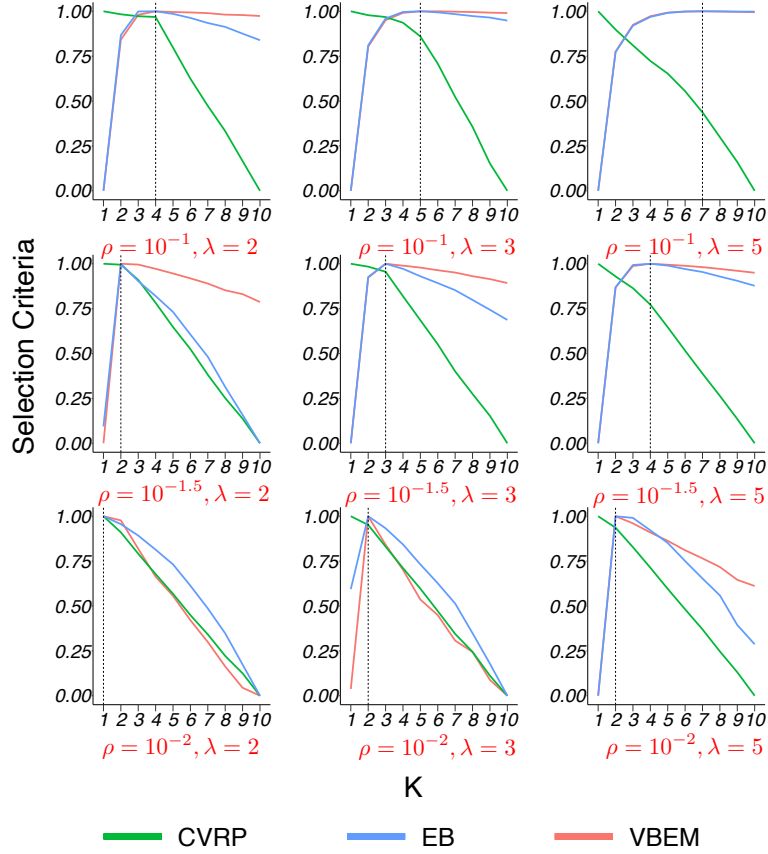


Figure S5 – Values of model selection criteria in model 4 simulation. Graph size (number of nodes) $n = 316$. With the graphon $W(x, y) = \rho\lambda^2(xy)^{\lambda-1}$, $\rho \in \{10^{-1}, 10^{-1.5}, 10^{-2}\}$ and $\lambda \in \{2, 3, 5\}$, the results for graphs with each set of parameters ρ and λ are shown in a panel. $\mathcal{I}_{\text{CVRP}}$, $\mathcal{I}_{\text{VBEM}}$, \mathcal{I}_{EB} are all standardized to $[0, 1]$, and $\mathcal{I}_{\text{CVRP}}$ is taken negative, thus the model is selected by the maximizer of each criterion. For the 100 graphs generated under each set of parameters, the values of three criteria are plotted against the input number of blocks $K = 1, \dots, 10$ used in clustering. The number of clusters selected by EB is highlighted by the dashed lines.